THE COMPTON-GETTING EFFECT FOR LOW ENERGY PARTICLES

F.M. Ipavich

University of Maryland, College Park, Maryland 20742

Technical Report #74-117

June 1974

UNIVERSITY OF MARYLAND
DEPARTMENT OF PHYSICS AND ASTRONOMY
COLLEGE PARK, MARYLAND

THE COMPTON-GETTING EFFECT FOR LOW ENERGY PARTICLES

F.M. Ipavich

University of Maryland, College Park, Maryland 20742

Technical Report #74-117

June 1974

Space Physics Group

THE COMPTON-GETTING EFFECT FOR LOW ENERGY PARTICLES

F. M. Ipavich

University of Maryland
College Park, Maryland 20742

ABSTRACT

The traditional first-order Compton-Getting effect, which relates particle distributions as observed in two frames of reference moving with constant relative velocity, is inadequate for the description of low energy particles (less than a few hundred keV/nucleon) in the solar system. An exact procedure is given for recovering both isotropic and anisotropic distributions in the solar wind frame from observations made in a spacecraft frame. The method is illustrated by analyzing a particle event observed by the University of Maryland experiment on IMP-7 on 31 October 1972.

INTRODUCTION

A distribution of particles which is isotropic in one frame of reference will display an anisotropy if observed from a different frame of reference. This is referred to as the Compton-Getting effect (Compton and Getting, 1935). For nonrelativistic particles the magnitude of the induced anisotropy (Gleeson and Axford, 1968; Forman, 1970) is equal to $(2 + 2\gamma)$ (w/v), where γ is the spectral index of the particle differential intensity, w is the relative speed of the two frames of reference, and v is the particle speed. The above formula assumes $w << v$. Recently Balogh, et al. (1973) have derived an expression for the anisotropy accurate to order $(w/v)^2$. For particle convection induced by the solar wind, w is equal to the solar wind speed. Present day satellite experiments respond to such low energies that the assumption $w << v$ can no longer be used. For example, one detector on the University of Maryland experiment on IMP-8 responds to heavy ions with energies $\sim$20 keV/nucleon (Tums, et al., 1974). Since v (km/sec) = 440 [E(keV/nucleon)]$^{1/2}$, this implies $v \simeq 5\ w$ for typical solar wind speeds, and $v \simeq 3\ w$ during disturbed periods. Future experiments will undoubtedly reach even lower energies.

In this letter we first derive an exact transformation of a particle distribution which is isotropic in the solar wind frame. We then show how a distribution with arbitrarily high anisotropy in the solar wind frame may be transformed exactly into the observer's frame. The procedure is illustrated by analyzing one of the "post-shock" particle spikes discussed by Gloeckler, et al (1974).

EXACT TRANSFORMATION FOR ISOTROPIC DISTRIBUTION

The exact transformation procedure is based on the Lorentz invariance of the particle distribution function in phase space (Forman, 1970). Let primed quantities refer to the solar wind frame and unprimed quantities to the observer's frame. All particles are assumed to be nonrelativistic, since for relativistic particles the first-order Compton-Getting correction is a perfectly good approximation.

The particle momenta in the two frames of reference are related by the Lorentz transformation

$$\vec{P}' = \vec{P} - P\,\vec{w}/v \quad . \tag{1}$$

Here $\vec{w}$ is the solar wind velocity and v is the particle speed. (Equation (1) assumes w << speed of light). The magnitudes of the momenta are related by

$$P' = P\,[1 - 2\,(w/v)\,\cos\,\Theta + (w/v)^2]^{1/2}, \tag{2}$$

where Θ is the angle between the solar wind velocity and the direction in which the observer is looking (i.e., $\cos\,\Theta = (\vec{w}\cdot\vec{P})/(wP)$).

The distribution function $f(\vec{P})$ is the number of particles of momentum $\vec{P}$ in the volume element dP_x, dP_y, dP_z, dx, dy, dz of phase space. As demonstrated by Forman (1970), this function is a Lorentz invariant:

$$f(\vec{P}) = f'(\vec{P}') \quad . \tag{3}$$

For the case of a distribution which is isotropic in the solar wind frame we have

$$f(\vec{P}) = f'(P') \quad . \tag{4}$$

If in addition the distribution function is a power law in the solar wind frame, $f'(P') \propto (P')^{-n'}$, then equations (2) and (4) may be combined to yield

$$f(\vec{P}) = f'(P) \; [1-2(w/v) \cos \Theta + (w/v)^2]^{-n'/2} \; . \tag{5}$$

It is apparent from equation (5) that the spectrum is not a power law in the observer's frame; both the shape and the intensity of the spectrum are functions of angle and energy. This may be seen quantitatively by computing an effective spectral index for a given momentum and angle as:

$$n_{eff}(P,\Theta) \equiv - \frac{d(\ln f)}{d(\ln P)} \quad . \tag{6}$$

Using equation (5) this becomes

$$n_{eff} = n' \; [\frac{1 - (w/v) \cos \Theta}{1 - 2 (w/v) \cos \Theta + (w/v)^2}]. \tag{7}$$

Introducing the particle differential intensity dJ/dE (particles per cm^2- sec - ster - keV) and using the relation $dJ/dE = P^2 f$ (Forman, 1970), it follows that if the distribution function is a power law in momentum, $f \propto P^{-n}$, then the differential intensity is a power law in kinetic energy, $dJ/dE \propto E^{-\gamma}$, with $\gamma = (n/2) - 1$. Thus, using equation (7), the effective

differential intensity spectral index is

$$\gamma_{eff} = \gamma' + \frac{(\gamma'+1)(w/v)\ [\cos\ \theta - (w/v)]}{1 - 2\ (w/v)\ \cos\ \theta + (w/v)^2} \quad . \tag{8}$$

Figure 1 shows γ_{eff} plotted vs. θ for (v/w) = 4 and 10, assuming a power law spectrum in the solar wind frame with $\gamma' = 3$. The steepest spectrum is seen when looking towards the sun ($\theta = 0°$).

Again using the relation $dJ/dE = P^2 f$ we obtain, using equation (5),

$$\frac{dJ}{dE} = \text{const} \times E^{-\gamma'}\ [1 - 2\ (w/v)\ \cos\ \theta + (w/v)^2]^{-(\gamma'+1)} \quad . \tag{9}$$

This differential intensity is plotted in Figure 2 for three values of θ assuming a solar wind speed of w = 400 km/sec and a spectral index $\gamma' = 3$ in the solar wind frame.

For small (w/v) we can expand equation (5) using $n = 2\gamma + 2$ to obtain, correct to order $(w/v)^2$,

$$f(\vec{P}) = f'(P)\ [1 + C\ (w/v) + D\ (w/v)^2] \quad , \tag{10}$$

where

$$C = 2(\gamma' + 1)\ \cos\ \theta$$

$$D = (\gamma' + 1)^2 + (\gamma' + 1)\ (\gamma' + 2)\ \cos\ 2\theta \quad .$$

Here C is the familiar first-order Compton-Getting correction. The second order term, D, has been obtained previously by Balogh, et al. (1973) by expanding equation (4) in a Taylor series.

EXACT TRANSFORMATION FOR ANISOTROPIC DISTRIBUTION

We describe both frames of reference using spherical coordinate systems with the polar axes along the sun earth line, and again use primes to denote quantities defined in the solar wind frame. Thus the momentum $\vec{P}$ in the observer's frame is labeled by magnitude P, polar angle Θ, and azimuthal angle ϕ. Since the azimuthal angles span planes which are normal to the solar wind velocity, it follows that $\phi = \phi'$ (i.e., in cartesian coordinates $P_x = P_x'$, $P_y = P_y'$). The change in the magnitude of momentum is given by equation (2). The polar angle Θ' must also be Lorentz-transformed (see e.g., Jackson, 1962):

$$\Theta' = \mathrm{Tan}^{-1} \left[\frac{\sin \Theta}{\cos \Theta - (w/v)} \right] \quad . \tag{11}$$

Thus equation (3) can be written quite generally as

$$f(P,\Theta,\phi) = f'(P[1-2(w/v)\cos\Theta + (w/v)^2]^{1/2},\ \mathrm{Tan}^{-1}\left[\frac{\sin\Theta}{\cos\Theta-(w/v)}\right],\phi) \quad . \tag{12}$$

In order to illustrate the use of equation (12), it is convenient to make a number of simplifying assumptions. Firstly, we assume that the detector system scans in the ecliptic plane so that the angle ϕ need not be considered. (It is a straightforward matter to consider different orientations.) Secondly, we assume that the distribution function in the solar wind frame is separable in the sense that

$$f'(\vec{P}') = g'(P')\ h'(\Theta') \quad . \tag{13}$$

This is probably a reasonable assumption over a limited energy range, although it should be noted that equation (2) implies even a detector responding only to an energy E_o will sample particle energies in the solar wind frame ranging from $[1 - (w/v)]^2 E_o$ to $[1 + (w/v)]^2 E_o$. Of course, if equation (13) does not allow a sufficiently good fit to the experimental data, a more general form must be used. Finally, we assume a power law spectrum with $g'(P') \propto (P')^{-n'}$. Now equations (5), (12), and (13) may be combined to yield the differential intensity seen in the observer's frame:

$$\frac{dJ}{dE} = \text{const} \times E^{-\gamma'} \left[1 - 2\,(w/v)\cos\theta + (w/v)^2\right]^{-(\gamma'+1)} \times h' \left\{\text{Tan}^{-1}\left[\frac{\sin\theta}{\cos\theta - (w/v)}\right]\right\} \quad . \tag{14}$$

APPLICATION

The use of equation (14) will be illustrated by analyzing one of the so-called "post-shock" spikes observed in interplanetary space by the University of Maryland experiment on IMP-7, and discussed by Gloeckler, et al. (1974) and Levy, et al. (1974). This particular sharp intensity increase lasted from 1954 to 1956 UT on October 31, 1972. The detector we are concerned with responds to alpha particles with energies between 95 and 135 keV/nucleon. The rate is sectored into four 90° sectors in the ecliptic plane, so that it is not possible to uniquely recover the function h' in equation (14). (This indicates the importance of additional

sectoring for future low energy experiments.) Instead, we must arbitrarily assume a form for h', numerically integrate equation (14) over four 90° sectors, and then compare the resultant four numbers with the four observed rates. Both observed and calculated rates are normalized to give an average rate of 50 for each sector; there are thus three independent rates to fit. We have assumed a two-parameter particle distribution in the solar wind frame of the form $h'(\theta') = 1 + b \cos(\theta' - \theta_o')$, with b representing the magnitude of the anisotropy and θ_o' its direction.

The solar wind velocity during this time was $w \simeq 700$ km/sec (H. Rosenbauer and H. Grunwald, private communication, 1974), so that $v \simeq 7w$. The <u>average</u> differential intensity spectral index, obtained from the observed intensities summed over all sectors for two detectors at different energies, was $\gamma = 3.0$ from $\sim$100 to 400 keV/nucleon. From Figure 1, we expect this average value to be approximately equal to the value in the solar wind frame, so we take $\gamma' = 3.0$. Thus the normalized rates obtained by integrating equation (14) depend on only <u>two</u> variables: b and θ_o'. Therefore, if the <u>three</u> independent observed rates can be fit, some confidence can be placed in the assumed form for h'. In this example, the best fit was obtained by choosing $b = 0.95$ and $\theta_o' = 146°$. In Figure 3 the dotted curve represents the assumed angular distribution of particles in the solar wind frame. The solid curve (obtained from equation (14)) represents the same distribution as viewed from the observer's frame. The normalized observed rate (with one sigma error) and the calculated rate are shown for each sector.

Since the agreement is really quite good, we conclude that our assumed form for h' is an accurate representation of the actual particle distribution in the solar wind frame during this event. Although the magnitude of the derived anisotropy is large (95%), the particle distribution is broad ($\Theta'_{FWHM} \simeq 177°$ in the solar wind frame). A more sharply peaked distribution cannot fit the data. This may be seen qualitatively by considering a delta function distribution in the solar wind frame: $h'(\Theta') = \delta(\Theta' - \Theta_o')$. Equation (14) shows that the distribution would also be a delta function in the observer's frame, $\delta(\Theta - \Theta_o)$. Equation (11) shows that for $\Theta_o' = 146°$, $\Theta_o \simeq 141°$. Thus the calculated rate would be 200 for sector 1, and zero for the other three sectors. This would obviously be a poor fit to the observed rates shown in Figure 3.

The average direction of the magnetic field in the ecliptic plane during this time period, observed on the same satellite, was $152° \pm 6°$ (shown by the arrow in Figure 3), where the variation represents real fluctuations in the field direction (N. Ness and R. Lepping, private communication, 1974). Thus the particle streaming was essentially field aligned with the particles coming from an easterly, anti-solar direction. From similar analyses, this same conclusion also holds for the other post-shock spikes described by Gloeckler, et al. (1974).

Acknowledgments. The author would like to thank G. Gloeckler, C. Y. Fan, and D. Hovestadt for the use of their particle data; N. Ness and R. Lepping for the use of their IMP-7 magnetic field data; and H. Rosenbauer and H. Grunwald for the use of their plasma data. This work was supported in part by NASA contract NAS5-11063.

REFERENCES

Balogh, A., S. Webb, and M. A. Forman, Higher order Compton-Getting anisotropies, Planet. Space Sci., 21, 1802, 1973.

Compton, A. H., and I. A. Getting, An apparent effect of galactic rotation on the intensity of cosmic rays, Phys. Rev., 47, 818, 1935.

Forman, M. A., The Compton-Getting effect for cosmic ray particles and photons, and the Lorentz-invariance of distribution functions, Planet. Space Sci., 18, 25, 1970.

Gleeson, L. J., and W. I. Axford, The Compton-Getting effect, Astrophys. Space Sci., 2, 431, 1968.

Gloeckler, G., F. M. Ipavich, C. Y. Fan, and D. Hovestadt, Post-shock spikes: a new feature of proton and alpha enhancements associated with an interplanetary shock wave, Geophys. Res. Lett., 1, 65, 1974.

Jackson, J. D., Classical Electrodynamics, p. 361, John Wiley and Sons, New York, 1962.

Levy, E. H., F. M. Ipavich, and G. Gloeckler, Possible acceleration of charged particles through the reconnection of magnetic fields in interplanetary space, submitted to Geophys. Res. Lett., 1974.

Tums, E., G. Gloeckler, C. Y. Fan, J. Cain, and R. Sciambi, Instrument to measure energy and charge of low energy interplanetary particles, IEEE Trans. Nucl. Sci., NS-21, no. 1, 210, 1974.

FIGURE CAPTIONS

Figure 1. Spectral index in the observer's frame as a function of direction assuming a spectral index $\gamma' = 3$ in the solar wind frame.

Figure 2. Differential intensity in the observer's frame for three different directions assuming a solar wind speed of 400 km/sec and an isotropic power law differential intensity in the solar wind frame with $\gamma' = 3$.

Figure 3. Angular particle distributions in the solar wind frame (dotted curve) and satellite frame (solid curve) deduced from observations of alpha particles (95-135 keV/nucleon) in a "post-shock" spike (1954-1956 UT October 31, 1972). The upper number in each bracket is the observed normalized counting rate (with one sigma error) for each sector, and the lower number is the calculated rate obtained by integrating the solid curve over that sector. The arrow indicates the average direction of the magnetic field in the ecliptic plane during this time period.

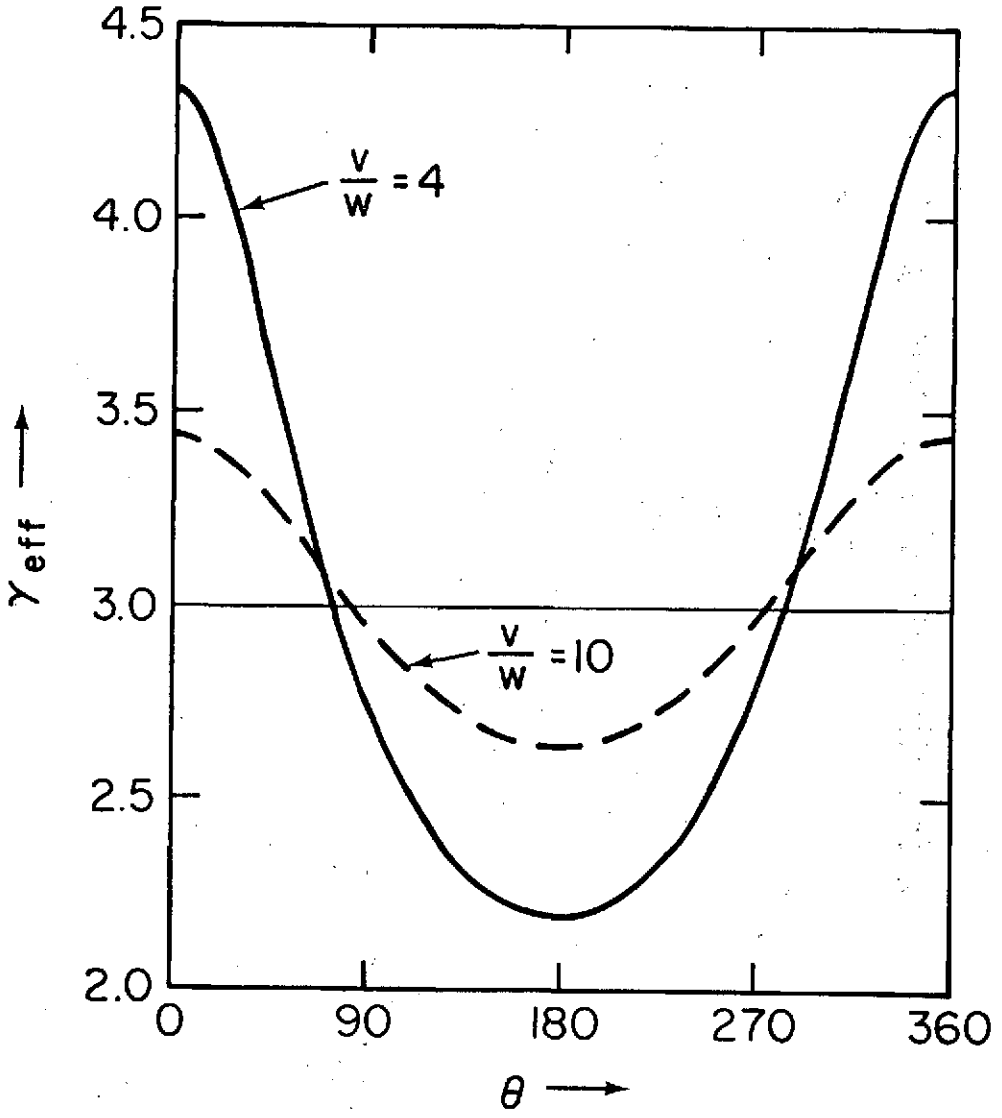
4.5
4.0
3.5
3.0
2.5
2.0
0
90
180
270
360
γ_{eff}
θ
$\frac{V}{W} = 4$
$\frac{V}{W} = 10$

Figure 1

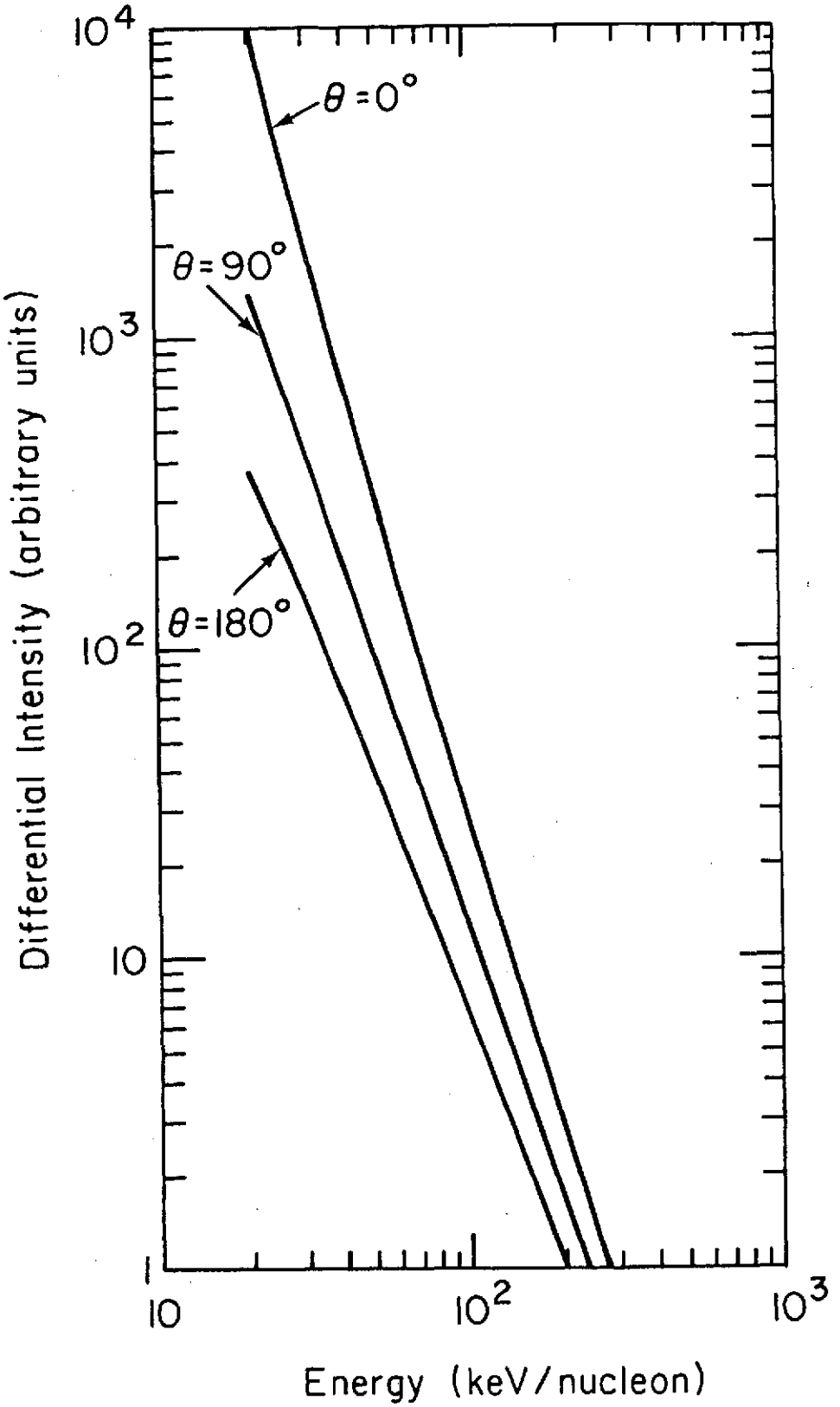
10^4
10^3
10^2
10
1
$\theta = 0°$
$\theta = 90°$
$\theta = 180°$
Differential Intensity (arbitrary units)
10
10^2
10^3
Energy (keV/nucleon)

Figure 2

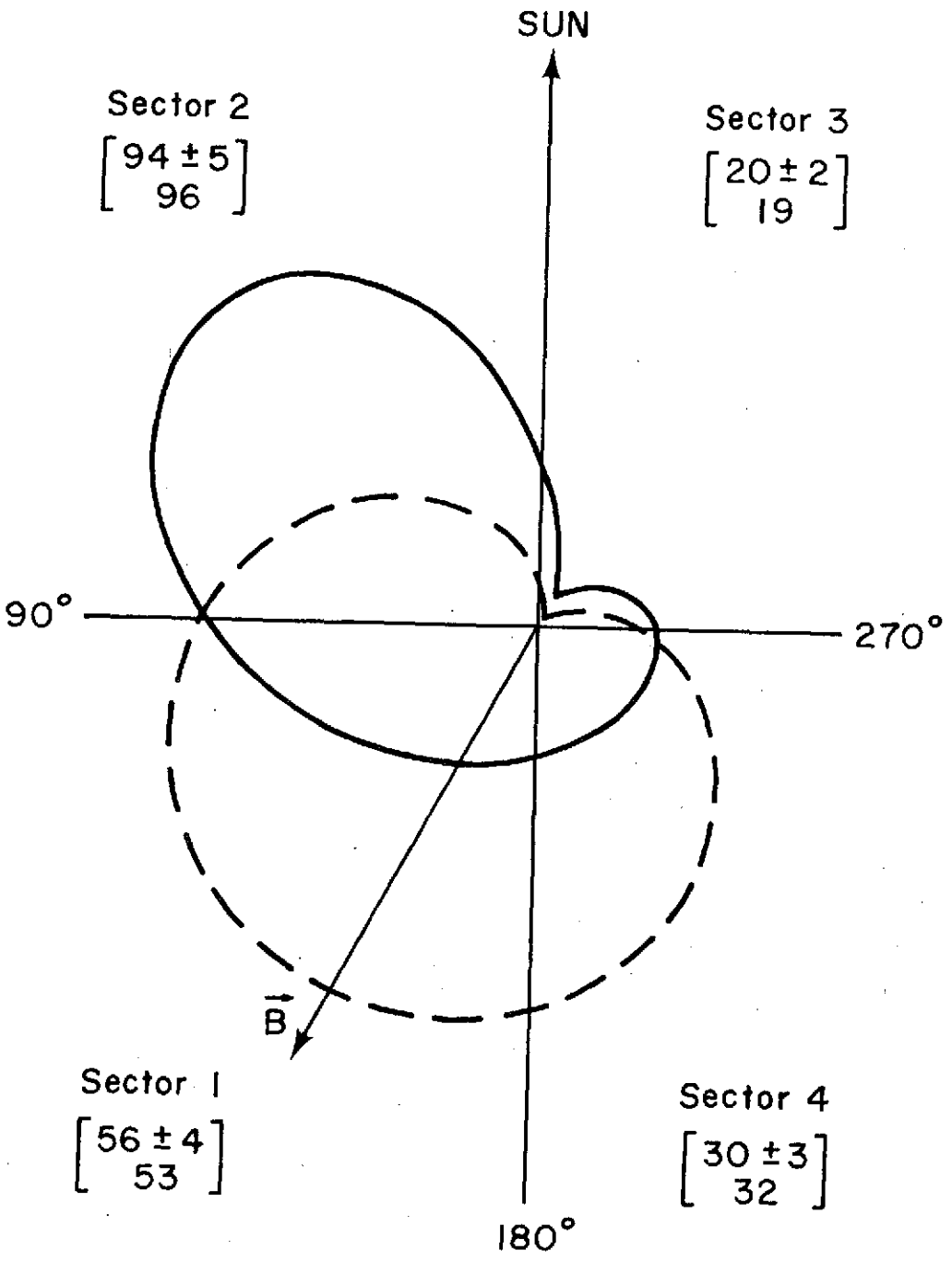
SUN
Sector 2
[94 ± 5
96]
Sector 3
[20 ± 2
19]
90°
270°
B
Sector 1
[56 ± 4
53]
Sector 4
[30 ± 3
32]
180°

Figure 3